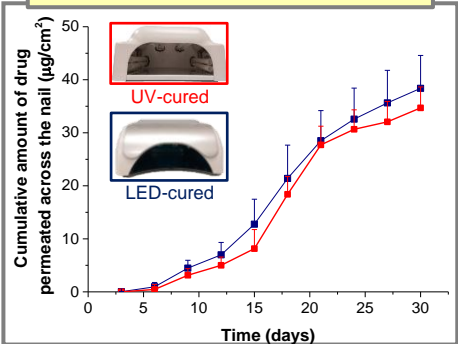
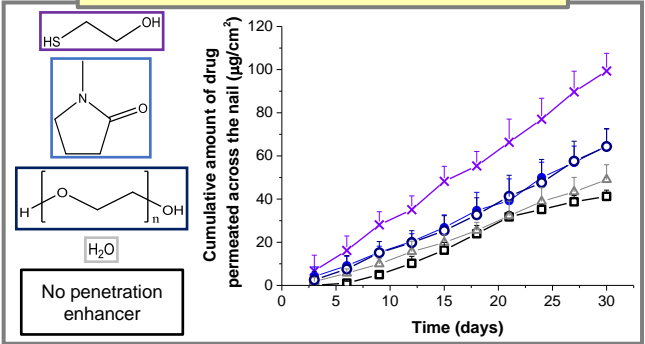


# \*Graphical Abstract (for review) UV-LED light

Ungual drug penetration from UV-curable gel formulations



## 2. Loaded with unguinal penetration enhancer



## **Two strategies to enhance unguinal drug permeation from UV-cured films: incomplete polymerisation to increase drug release and incorporation of chemical enhancers**

Laxmi Valji Kerai, Josep Bardés, Stephen Hilton, Sudaxshina Murdan\*

UCL School of Pharmacy, 29-39 Brunswick Square, London, WC1N 1AX, UK

\*Corresponding author

T +44-207 753 5810

E [s.murdan@ucl.ac.uk](mailto:s.murdan@ucl.ac.uk)

## ABSTRACT

UV-curable gels, which polymerise into long-lasting films upon exposure to UVA, have been identified as potential topical drug carriers for the treatment of nail diseases. Limitations of such films include incomplete drug release and low ungual drug permeation. The aim of the work herein was therefore to investigate two strategies, namely: (1) increasing drug release from the film, and (2) increasing nailplate permeability, with the ultimate goal of enhancing ungual drug permeation. To increase drug release via Strategy 1, a UV-LED lamp (whose emitted light was suboptimal for gel polymerisation) was used, and it was hypothesised that such a lamp would result in films that are less polymerised/cross-linked and where the drugs are less 'trapped'. Indeed, the suboptimal lamp influenced polymerisation, such that the films were thinner, had lower glass transition temperatures and enabled a slightly greater (by 15%) drug release of one of the two drugs tested. However, the greater drug release had only a modest impact on ungual drug permeation. To evaluate Strategy 2, i.e. increase nailplate permeability, chemical ungual enhancers, 2-mercaptoethanol (ME), 2-methyl pyrrolidone (NMP), PEG 200 and water were incorporated within the UV-cured films. These chemicals caused increased ungual drug permeation, with ME showing the greatest (by 140%), and water showing the least (by 20%) increase in the amount of drug permeated by day 30. Surprisingly, these chemicals also caused increased drug release from the films, with ME once again having the greatest effect (by 51%) and water the least effect (by 12%). It seems that these chemicals were increasing ungual drug permeation via their influence on drug release (i.e. via their impact on the film) as well as via their influence on the nail itself. We conclude that, of the two strategies tested, the second strategy proved to be more successful at enhancing ungual drug permeation.

Keywords: nail, ungual, drug release, drug permeation, UV-curable gels, topical, UV LED lamp

## 1. Introduction

While the healthy nail unit is usually considered a cosmetic organ, especially by women, and manicuring has a long history (Shapiro, 2014), disorders of the nail unit are common, and can affect some or all the parts of the nail apparatus (Rich and Scher, 2003). For example, only the paronychia tissues may be affected, or the nail plate's shape, colour, surface, mechanical properties and attachment to the underlying soft tissues may be altered (Murdan, 2012). Onychomycosis (fungal infections of the nail) and nail psoriasis are the two most common nail disorders and share other similarities, for example, they are of long duration, are difficult-to-treat conditions, and have a significant impact on the quality of life of sufferers (Arrese and Pierard, 2003; Milobratovic et al., 2013; Ortonne et al., 2010). For many sufferers, treatment is important, and topical therapy would be ideal for its avoidance of systemic adverse effects and of drug interactions. However, currently available topical medicines for onychomycosis and nail psoriasis have low efficacies (Murdan, 2016; Thomas et al., 2010). Consequently, much research is being conducted on the formulation of more effective topical therapeutics, e.g (Delgado-Charro, 2015; Elsayed, 2015; Kushwaha et al., 2015) and a range of formulations such as lacquers, films, solutions, hydrogels, patches, microemulsions and liposomes have been investigated (Saner et al., 2014; Shivakumar et al., 2012).

Recently, a formulation, UV-curable gels, was borrowed from the nail cosmetic industry, and investigated for pharmaceutical application (Kerai et al., 2016; Kerai et al., 2015). UV-curable gels composed of diurethane dimethacrylate (DUDMA), a reactive (meth)acrylate monomer such as ethyl methacrylate or 2-hydroxyethyl methacrylate) or iso-bornyl methacrylate, the polymerisation photoinitiator 2-hydroxy-2-methylpropiophenone, ethanol and an anti-onychomycotic drug (amorolfine HCl or terbinafine HCl) were formulated. Upon gel exposure to a UVA lamp, the photoinitiator absorbs UVA and is cleaved into free radicals, which initiate polymerisation reactions among DUDMA and the methacrylate monomers, which leads to gel curing into a film. These aesthetically- and pharmaceutically- acceptable, visually smooth and transparent films had a long residence *in vivo* in humans, were stable over months at ambient conditions, and enabled drug

permeation into and through the nail at sufficient levels to show *in vitro* anti-fungal activity. However, drug release from the films was incomplete over the 30-day experiment, being a maximum of 50% for amorolfine HCl and 30% for terbinafine HCl. Ungual drug permeation into and through the nail plate was low for both drugs, being less than 7% (of the applied dose) for amorolfine HCl and less than 5% for terbinafine HCl.

Such incomplete drug release from the films and low unguinal drug permeation are potential limitations of the UV-curable formulations. Drug release may become a rate-limiting step if insufficient drug is available for unguinal permeation. In turn, low levels of drug permeating into the nail plate could limit fungal kill and formulation efficacy. The **aim** of the work described in this manuscript was therefore to investigate two strategies for enhancing unguinal drug permeation, namely: i) increasing drug release from the films and ii) increasing nailplate permeability to topically-applied drugs.

It was hypothesised that drug release from the film could be increased by influencing the gel polymerisation process, specifically by allowing polymerisation to occur to an incomplete extent, such that the formed film would be less cross-linked and the drug would be less 'trapped' within it. To test the hypothesis, two UVA lamps were used, a traditional UVA lamp (which emits UVA in the range of 320–400 nm) and a UV-LED lamp (which emits light at 350-375 nm). The LED lamp was expected to cause incomplete polymerisation due to its light being suboptimal for the selected photoinitiator, 2-hydroxy-2-methylpropiophenone, which has UV absorbance peaks at 245, 280 and 331 nm (Schwalm, 2007). Exposure of the photoinitiator to a lower level of UVA from the LED lamp was thus expected to reduce the extent of gel polymerisation and the formation of a film where the drug was less 'trapped'.

For the second strategy, chemicals which have been shown to act on the nail plate and enhance unguinal drug permeation were incorporated into the UV-curable gel formulations. It was hypothesised that following topical application of the gels, exposure to UVA and formation of a film on the nail, the chemical unguinal enhancers would be released from the

film, enter and act on the nail plate to increase the latter's permeability, which would result in increased unguis permeation of the drug. Four unguis enhancers, namely, 2-mercaptoethanol (ME), water, 1-methyl-2-pyrrolidinone (NMP) and PEG 200 (properties shown in Supplementary material 1), which act via different mechanisms, were selected. The thiol, ME, enhances unguis drug permeation by reducing the disulphide bonds of the nail keratin, and thereby disrupting the integrity of the nail plate barrier:



Thiols seem to be the most effective of unguis penetration enhancers investigated so far, and ME was found to be the most potent when compared to other thiols, N-acetylcysteine and thioglycolic acid (Patel and Vora, 2016). In contrast to the thiol, water, NMP and PEG 200 do not disrupt the disulfide bonds responsible for the integrity of nail keratin. Instead, these chemicals increase nailplate swelling, which can facilitate unguis drug diffusion (Ahn et al., 2013; Gunt and Kasting, 2007; Hossin et al., 2016; Nair et al., 2010; Walters and Flynn, 1983).

**Note** that the gel formulations used to evaluate the two strategies were different formulations. Strategy 1 was tested using formulations where ethyl methacrylate (EMA) was the reactive monomer, while Strategy 2 was tested using formulations where 2-hydroxyethyl methacrylate (HEMA) was the reactive monomer. The experiments involved with Strategy 1 were conducted first, and by the time Strategy 2 was tested, other work in our laboratory had shown that HEMA formulations were superior to EMA formulations, enabling a greater drug load, drug release from the films and unguis drug permeation (Kerai et al., 2016). Thus, the optimal HEMA formulations were chosen for Strategy 2.

For both strategies, amorolfine HCl (AH) and terbinafine HCl (TH) were selected as the drugs for loading into the films. Terbinafine HCl is the oral anti-onychomycotic drug of choice in the UK and much research effort is ongoing to produce a topical anti-onychomycotic preparation. Amorolfine HCl is the drug whose topical formulation (Loceryl® nail lacquer) has been the most effective topical preparation for many years, prior to the FDA-approval of Kerydin® and Jublia® in 2014. A more effective formulation of amorolfine HCl is needed,

given that the cure rate of Loceryl has been reported to be between 13 and 52% (Murdan, 2016). Use of both drugs in this study also allows us to determine an effect of drug nature, if any, on the two tested strategies.

## **2. Materials and methods**

### **2.1. Materials**

Amorolfine HCl was purchased from Ranbaxy Research Laboratories (Haryana, India) and terbinafine HCl from AK Scientific (CA, USA). Diurethane dimethacrylate, EMA, HEMA, 2-hydroxy-2-methylpropiophenone, absolute ethanol, methanol, mercaptoethanol, NMP, propan-2-ol, triethylamine, phosphoric acid 85% wt. solution in water and trifluoroacetic acid were purchased from Sigma–Aldrich (Dorset, UK). Acetonitrile HPLC gradient grade and PEG 200 were purchased from Fisher Scientific (Hertfordshire, UK and Loughborough, UK respectively). A 36 W Cuccio Professional UVA nail lamp was purchased from Amazon UK and a 36 W Professional Salon Quality 18 K UV-LED nail lamp was purchased from eBay UK. Nail & Beauty Emporium super absorbent lint-free wipes (4 ply) were purchased from Just Beauty UK, an online retailer specialising in professional beauty, hair and skin products. Healthy human nail clippings (fingernails) were obtained from male and female volunteers aged between 18 and 65 years following ethics approval (REC/B/10/01 School of Pharmacy, University of London, UK).

### **2.2. Preparation of UV gels and films**

#### **2.2.1. Preparation of formulations to study the influence of the nature of the UVA lamp**

Gels composed of DUDMA and EMA at a 85:15% v/v ratio, 2-hydroxy-2-methylpropiophenone at 3% v/v of the gel mixture, ethanol at 25% v/v of the gel mixture, and either 3% w/v AH or 4% w/v TH were used. These formulations were prepared by first dissolving the drug in ethanol, and then adding DUDMA, EMA and the photoinitiator and stirring the mixture overnight to produce a clear homogenous solution. To prepare the films, the gel mixture was applied on a microscope glass slide using a pipette tip (30 µl to an area

of 15 mm x 15 mm in a single layer), and the glass slide was placed under either a UV-LED lamp or a traditional UV lamp for two minutes. This caused gel polymerisation and formation of a film. The surface of the film was wiped with propan-2-ol using a nail wipe to remove the oxygen inhibition layer (an unreacted monomer layer). This revealed a transparent polymer film, which was then removed from the glass slide using a scalpel and used in film characterisation experiments as described in Section 2.3. Note, for unguinal permeation experiments, the gels were cured directly on the dorsal surface of nail clippings (rather than on microscope slides).

### **2.2.2. Preparation of formulations containing unguinal penetration enhancers**

Gels composed of DUDMA and HEMA, 2-hydroxy-2-methylpropiophenone, ethanol, and either AH (at 4% w/v) or TH (at 6% w/v) were used to investigate the effect of incorporating chemical enhancers on unguinal drug permeation. Five types of formulations were prepared containing either (i) no penetration enhancer (the control), (ii) water, (iii) ME, (iv) NMP or (v) PEG 200. The ethanol and penetration enhancer together made up no more than 25% v/v of the gel, so that the incorporation of the penetration enhancer would not adversely affect: i) gel viscosity (which was typically between 22-23 mPas at 25°C), and thereby gel applicability on the nail, and ii) the films formed after polymerisation. Details of the gel compositions are shown in Table 1.

The formulations (except where ME was the enhancer) were prepared by mixing ethanol and enhancer, dissolving the drug in this mixture, and then adding DUDMA, HEMA and the photoinitiator and stirring the mixture overnight to produce a clear homogenous solution. The films were prepared as described in Section 2.2.1 using the traditional UVA lamp (which emits UVA in the range of 320–400 nm). ME-containing formulations were prepared similarly, except that ME was incorporated immediately prior to UV exposure in order to prevent premature polymerisation. It was observed that formulations containing ME polymerised even in the absence of UVA application.

The concentration of the penetration enhancer in the gel was the maximum that could be incorporated while ensuring that the drug remained in the dissolved state. A maximal

enhancer concentration was sought, given that unequal drug permeation increases with increasing enhancer concentration (Patel and Vora, 2016). In order to determine the highest concentrations of enhancer that could be used, gels containing DUDMA, HEMA, the photoinitiator, the antifungal drug and penetration enhancers at 2.5, 5, 7.5, 10 or 12.5 % v/v with corresponding ethanol concentrations at 22.5, 20, 17.5, 15 or 12.5 % v/v were prepared. These formulations were visually observed, exposed to UV light and the resulting films were examined by polarised light microscopy and X-ray diffraction. The results showed that enhancer concentrations of 10% v/v for water and 5% v/v for ME, NMP and PEG 200 produced films where the drug remained in the dissolved state while higher concentrations resulted in films containing drug crystals.

### **2.3. *In vitro* characterisation of the gels and resulting UV-cured films**

The *in vitro* properties of the gels and of the films were determined as described below and as previously reported in (Kerai et al., 2016; Kerai et al., 2015).

#### **2.3.1 Gel-to-film mass yield**

The percentage mass conversion from monomer mixture to polymer film was calculated using the following equation:

$$\text{Yield (\%)} = (W_t/W_0) \times 100$$

where  $W_0$  is the weight of the monomer mixture before curing and  $W_t$  is the weight of the UV-cured film.

#### **2.3.2 Fourier Transform Infrared (FT-IR) Spectroscopy to determine degree of polymerisation**

During polymerisation, alkene bonds are converted to alkane ones. The reduction in alkene bonds upon curing from monomer mixture to polymer film was therefore taken as an indicator of polymerisation, using FTIR. Spectra of the uncured and cured formulations were obtained using the OPUS 7.0 software and recorded by a Bruker Alpha IR Spectrophotometer (Bruker Corporation, Germany), using 24 scans over the 400 – 4000  $\text{cm}^{-1}$  range with background subtraction. The % degree of conversion (DC) was calculated from the ratio of the height of the absorbance peak of the aliphatic C=C bond (1636  $\text{cm}^{-1}$ ) relative

to that of the carbonyl group ( $>C=O$ ,  $1702\text{ cm}^{-1}$ ), used as an internal standard, using the following equation:

$$DC (\%) = \frac{(A_{1636}/A_{1702})_0 - (A_{1636}/A_{1702})_t}{(A_{1636}/A_{1702})_0} \times 100$$

where  $(A_{1636}/A_{1702})_0$  and  $(A_{1636}/A_{1702})_t$  are relative absorbance of C=C bonds to C=O before curing and after curing respectively.

**2.3.3** The **thickness** of the films was measured using a Sealey AK9635D 0-25 mm Digital External Micrometer (PVR Direct, UK). Each film was measured at three separate points to obtain an average and precautions were taken to avoid compressing the film.

**2.3.4 Film microstructure** was examined by Scanning Electron Microscopy. The samples were gold sputter coated (10 nm) and imaged using FEI Quanta 200F (Eindhoven, The Netherlands).

**2.3.5** The **state (crystalline/amorphous)** of the drug within the films was determined using Polarised Light Microscopy (PLM) and X-Ray Diffraction (XRD). Films were examined by PLM for the absence/presence of drug crystals using a Nikon Microphot-FXA microscope (Nikon Corporation, Tokyo, Japan) and polarising filters. Images were taken using a Lumenera Infinity 2 digital camera (Lumenera Corporation, Ottawa, Canada) attached to the microscope. X-ray diffraction spectra of the antifungals and of the polymer films were obtained using a Rigaku MiniFlex 600 X-ray diffractometer (Rigaku Corporation, Tokyo, Japan) equipped with MiniFlex Guidance software. The samples were scanned over an angular range of  $2 - 60^\circ$ , with a step size of  $0.02^\circ$  and step duration of  $0.5^\circ/\text{min}$ . The generator voltage was set at 40 kV and the current at 15 mA. The data was analysed using OriginPro 9.0.

**2.3.6** The **levels of residual monomers** in the polymer film were quantified by ultrasonic extraction. Immediately after curing, one gram of each film was placed in a glass vial and three millilitres of methanol was added. The mixture was sonicated for up to 2 hours. Subsequently the solvent was analysed using Gas Chromatography to quantify the extracted residual monomers. GC was conducted using a 7890A GC System (Agilent, USA) equipped

with a flame ionisation detector (FID) system. Chromatographic separation was achieved on a HP-5 column (30 m long x 320 µm inside diameter with 0.25 µm film thickness). The sample injection volume was 2 µl. The injector was in the split mode (100:1) and its temperature was maintained at 250 °C throughout the experiments. The column temperature was raised from 45 °C (hold 2 min) to 110 °C (hold 2 min) at a 10 °C/min heating rate to 280 °C (hold 2 min) at a 20 °C/min heating rate. The flow rate of carrier gas (N<sub>2</sub>) was 1.5ml/min. The detection was carried out by the FID with the temperature of 280 °C and the ratio of H<sub>2</sub>/air at 25/250. The method developed was validated for linearity, precision and accuracy.

**2.3.7** The film's **glass transition temperature** was determined using Differential Scanning Calorimeter (DSC), using the Q2000 TA Instruments (Waters LLC, Delaware, USA), equipped with TA Universal Analysis 2000 software. Oxygen-free nitrogen gas with a purge rate of 50 ml/min was used. Approximately 8 mg of sample was contained within a T-zero pan following seal with a T-zero hermetic lid. Each sample was heated from -30 °C to 250 °C with a heating rate of 10 °C/min.

**2.3.8** The **drug-load** in UV-cured polymer films was determined by ultrasonic extraction using a Transonic T460/H sonicator (Elma, Germany). Ten milligrams of each film was placed in a glass vial. Five millilitres of ethanol was added to the film and the vial was sonicated for up to 2 hours. Subsequently the solvent was analysed by HPLC (as described in section 2.3.11).

**2.3.9 Drug release from films** was measured using Franz diffusion cells, and the drug-loaded films were supported on a cellulose membrane. The receptor fluid was a 0.1 M phosphate buffer at pH 5 as both amorolfine HCl and terbinafine HCl are stable at this pH (Hossin, 2015). Sink conditions were maintained throughout the duration of the study. To set up the Franz cell, a dialysis tubing cellulose membrane was cut into a circle with an area of 4.909 cm<sup>2</sup>. A test formulation was then applied onto the surface of the cellulose membrane, covering a circular area of 0.9503 cm<sup>2</sup>. The cellulose membrane was placed under a UVA lamp and the formulation was cured for two minutes. The surface of the film produced was then wiped with propan-2-ol using a nail wipe. The cellulose support with the UV-cured film

was then placed between the donor and receptor compartments of a Franz diffusion cell, with the test films facing the donor side, and the compartments were clamped together. Subsequently, four ml of receptor fluid was added to the receptor compartment while ensuring that no air bubbles were introduced. The diffusion cells were left to stir on a magnetic stirrer placed in a water bath maintained at 32 °C. Samples of the receptor fluid were collected at pre-determined time intervals for 30 days. Half ml was collected via the receptor arm and replaced with 0.5 ml of fresh buffer at each sampling point. The samples were analysed by HPLC (as per section 2.3.11) to determine the amount of drug released, and the cumulative % drug release over time was plotted. The UV-cured films were also observed by polarised microscopy prior to the release study and at day 30 to determine if there was any drug crystallisation and precipitation out of the film during the release study.

### **2.3.10 *In vitro* unguinal drug permeation**

Modified Franz diffusion cells were used. Human fingernail clippings were obtained from healthy volunteers aged between 18-65 years, washed with water and soaked in distilled water for one hour prior to use. They were then cut to size (circular, with a diameter of 0.3 cm) and measured for thickness using a micrometre. The formulation (2 µl) was applied on the nail surface and cured under a lamp for two minutes. The surface of the film produced was then wiped with propan-2-ol using a nail wipe. The nail was placed in the donor compartment and fixed into place, such that when assembled with the receptor compartment, the under-surface of the nail alone was exposed to the receptor fluid. The area exposed was 0.025 cm<sup>2</sup>. Subsequently, 900 µl of receptor fluid was added to the receptor compartment. The receptor fluid was 0.1 M phosphate buffer pH 5. The diffusion cell was assembled, covered with parafilm, and left to stir on a magnetic stirrer placed in a water bath at 32 °C. Samples of the receptor fluid were collected over 30 days by taking 50 µl of receptor fluid for analysis via the receptor arm and replacing it with 50 µl of fresh buffer. The samples were analysed by HPLC (as per section 2.3.11) to determine the amount of drug permeated across the nail over time. Each experiment was repeated six times. The cumulative amount of antifungal drug permeated through the nail (µg/cm<sup>2</sup>) (Q) against time (t) was plotted and the steady-state flux (J) was calculated from the slope of the linear portion of the plot (day 12 to day 24) as follows:

$$J = \Delta Q / \Delta t$$

The apparent permeability coefficient (P) which is defined as the flux divided by the concentration of the permeant in the donor compartment ( $C_d$ ) was calculated using:

$$P = J/C_d$$

The transport lag time ( $t_L$ ) was estimated by extrapolating the linear portion of the Q versus t plot to the x-axis, (i.e. the x-intercept), and the effective diffusion coefficient ( $D_{eff}$ ) was obtained from the transport lag time by the relationship:

$$t_L = h^2/6D_{eff}$$

where h represents the thickness of the nail plate, as per (Williams, 2003).

At the end of the permeation study, the nail clipping was removed from the donor compartment using forceps. The film on the nail surface was carefully lifted off the nail using a scalpel and placed in a vial containing 1 ml of ethanol. The mixture was ultrasonicated for 2 hours and the solvent was analysed by HPLC to quantify the amount of drug remaining in the donor compartment. The nail plate was rinsed with distilled water and blotted dry with Kimwipes, before placing in a vial containing 1ml of ethanol. This was ultrasonicated for 2 hours and the solvent was analysed with HPLC while the nail clipping retrieved was placed in another vial containing 1 ml of ethanol for a further two hour sonication. This extraction procedure was repeated until no further drug was extracted. The total amount of drug extracted from the nail was then calculated.

### **2.3.11 High-performance liquid chromatography (HPLC)**

The amount of amorolfine HCl and terbinafine HCl in samples was quantified by using a 1260 Infinity Agilent HPLC system equipped with an autosampler and a variable wavelength absorbance detector (Agilent Technologies, Germany). Elution was performed using a Luna C18 column (150 x 4.6 mm, 5  $\mu$ m) at a temperature of 40 °C. For amorolfine HCl, the mobile phase was 0.1% trifluoroacetic acid: acetonitrile (55:45 v/v), flow rate was 1.0 ml/min, sample injection volume was 20.0 $\mu$ l, wavelength was 220 nm and retention time was 5.8 minutes. For terbinafine HCl, the mobile phase was 0.012M triethylamine + 0.020M phosphoric acid: acetonitrile (65:35 v/v), flow rate was 1.0 ml/min, sample injection volume was 20.0 $\mu$ l, wavelength was 224 nm and retention time was 8.8 minutes. The method had been validated for linearity, precision and accuracy (Hossin, 2015)

## **2.4 Measurement of temperatures reached in the 2 lamps during operation**

The temperatures reached in the UV-LED and traditional UV lamps was measured with an Infrared thermometer (RS-1327, range -35°C - +500°C, RS Components Ltd., UK), to determine the temperatures that formulations are exposed to during polymerisation. This was to establish whether any differences in the heat generated by the two lamps could contribute to differences (if any) in gel polymerisation and properties of the resulting films. To monitor the temperature, the lamp was switched on and the temperature at a specific point inside the lamp (where the UV-curable gel would usually be placed for polymerisation) was measured at times 0, 10, 20, 30, 40, 50, 60, 70, 80, 90, 100, 110 and 120 seconds.

## **2.5. Statistical analysis**

All the experiments described above were repeated three times (with the exception of the unguinal drug permeation which was repeated six times). Statistical calculations were conducted using IBM SPSS 22 software. The data was tested for Normality using the Shapiro-Wilk test and then analysed using either a t-test (for Normally-distributed data) or Mann-Whiney U test (for non-Normally-distributed data) when comparing two groups. For multiple group comparisons, ANOVA followed by Tukey (for Normally-distributed data) or the Kruskal Wallis test followed by Nemenyi's test (for non-Normally-distributed data) were conducted. Repeated measures ANOVA was conducted to determine whether there were differences in the temperature profiles of the two lamps, and in the drug release and unguinal drug permeation profiles of the formulations.

## **3. Results**

### **3.1. Influence of the nature of the lamp**

#### **3.1.1. Influence of the emitted light on the polymerisation process and on the film formed**

The polymerisation pathway has been described previously (Kerai et al., 2015) and is schematically shown in Supplementary material 2. Upon gel exposure to a UVA lamp, polymerisation is initiated when the photoinitiator absorbs UVA and is cleaved into free radicals. The benzoyl radical reacts with an alkene group in DUDMA forming another free radical, which reacts with the alkene group in EMA forming another free radical, which reacts with an alkene group in another DUDMA molecule, and so forth, such that a cross-linked polymer network is ultimately produced. Each DUDMA molecule contains two alkene groups, one or both of which can be involved in the polymerisation reactions, and thereby be converted into alkane groups.

Following exposure to a UVA lamp and conversion of a gel formulation into a film, the surface of the latter was wiped with an isopropanol-soaked wipe to remove the oxygen inhibition layer (an unreacted monomer layer that is formed at the surface of the polymer film, where polymerisation is inhibited by atmospheric oxygen (Draelos, 2010; Schoon, 2005) to reveal a transparent polymer film. Removing the oxygen inhibition layer results in a loss of mass, such that the gel to film mass yield is less than 100%, as shown in Table 2 for both lamps. A significantly lower gel to mass yield (by about 18%,  $p < 0.05$ ) for the UV-LED lamp indicates a greater removal of mass, i.e. a greater amount of unreacted monomer layer. This, in turn, led to the UV LED-cured films being thinner (by around 18%,  $p < 0.05$ ).

Although thinner, the UV-LED cured films were visually similar to those produced by the traditional UV lamp. This suggests that the photoinitiator in the gel absorbed sufficient photons from the UV-LED lamp to initiate polymerisation reactions. Consequently, the extent of polymerisation (indicated by the degree of alkene-to-alkane conversion in the film, was similar ( $p > 0.05$ , Table 2) as were the levels of residual EMA reactants in the films ( $p > 0.05$ ). In contrast to EMA, the levels of DUDMA were higher by about 30% in the LED-cured films ( $p < 0.05$ ). Despite the statistical significance of the higher DUDMA levels, the levels of residual reactants in the films were still very low in all the films, which suggest that the less than 100% alkene-to-alkane degrees of conversion during polymerisation (Table 2) are due to unreacted alkene groups of DUDMA (which contains two polymerisable C=C bonds) within the polymer network, rather than due to unreacted monomers. Indeed the

values for the alkene to alkane conversion are in line with those reported (i.e. 43-73%) for photo-activated methacrylate-based dental composites (Halvorson et al., 2003).

The films produced by the two lamps were also similar in a range of other parameters. For example, both polymer films cured by LED or traditional UV lamps had high uniformity of thickness ( $\geq 95\%$ ) and similar smooth and transparent visual appearances, FT-IR spectra (Supplementary material 3), X-ray diffractograms and polarised light micrographs (Supplementary material 4) which indicated an amorphous nature and absence of drug crystals, scanning electron micrographs which showed a dense interior (Fig. 1) and drug concentrations which were similar to those in the corresponding gels (Table 2,  $p>0.05$ ). Similar drug concentrations in gels and films showed the drug did not preferentially migrate to the film surface or interior during polymerisation with either lamp. In contrast to these similarities, the glass transition temperatures of the LED-cured films were lower by about 10% (Table 2,  $p<0.05$ ).

### **3.1.2 Influence of lamp on drug release from the film**

Drug release from the films is shown in Figure 2. It can be seen that, for both drugs, a burst release occurred during the first 24 hours (due to drug release from the film surface), followed by a slower rate of release until a plateau was reached, which was well below 100% of the total drug load in the film. Examination of the films at the end of the experiments showed negligible change in film mass and an absence of drug crystals. Thus, drug precipitation in the film during the experiment was ruled out as a possible cause of the incomplete drug release. Rather, it seems that the film's cross-linked nature and dense microstructure (Fig. 1) limit the movement of drug molecules through and out of the film. Fitting of the release data using zero order, first order and Higuchi models showed the best fit to be the Higuchi model ( $r^2\geq 0.95$ ), which indicates that the drug release following the initial burst was diffusion-controlled.

Figure 2 also shows that terbinafine HCl was released to a much lesser extent compared to amorolfine HCl. The lower release of terbinafine HCl from UV-cured films reflects previous findings (Kerai et al., 2016; Kerai et al., 2015), and the work herein shows that the lower release of terbinafine HCl was maintained when the gel was cured using an LED lamp. It is unclear why terbinafine release is about half that of amorolfine; the two drugs have similar log P values (5.8 and 5.3 for amorolfine HCl and terbinafine HCl respectively) and molecular weights (353.97 and 327.89 Da for amorolfine HCl and terbinafine HCl respectively). A low drug release could occur if terbinafine was incorporated in the polymer structure upon UV-curing or if terbinafine has a higher affinity to the polymer film compared to amorolfine, which would hinder its release.

When the influence of the lamp on drug release is examined, it can be seen that drug release was higher from the films cured by the UV-LED lamp compared to the corresponding films cured by the traditional UV lamp; however statistical significance was only achieved for amorolfine HCl, from day 15 onwards (Mann Whitney test,  $p < 0.05$ ).

### **3.1.3 Influence of lamp on unguinal drug permeation**

The influence of the lamp on unguinal permeation is shown in Figure 3, and calculated unguinal drug permeation parameters are shown in Table 3. From Fig. 3, it can be seen that LED-cured films showed slightly greater unguinal drug permeation compared to the corresponding films cured with the traditional UV lamp over the 30-day experiment, although statistical significance was not reached (repeated measures ANOVA,  $p > 0.05$ ). However, the LED lamp did cause significantly reduced lag time and increased drug-in-nail levels at the end of the experiment for amorolfine HCl (Table 3, also seen in the inset of Fig. 3 as % drug in nail, which was  $4.3 \pm 1.3$  vs  $1.8 \pm 0.9$ , t test,  $p < 0.05$ ). For terbinafine HCl, the LED lamp increased the diffusion coefficient (t test,  $p < 0.05$ ) and the % of drug that permeated through the nail (seen in the inset of Fig. 3, which was  $1.1 \pm 0.3$  vs  $0.8 \pm 0.1$ , t test,  $p < 0.05$ ). Thus, the LED lamp increases unguinal drug permeation to some extent, although the influence is small and

most of the unguinal permeation parameters were similar for the UV-LED and the UV-cured films (Table 3). Mass balance was 97.0-99.9% (Supplementary material 5).

When the two drugs are compared, terbinafine HCl showed lower unguinal permeation (Fig.3, repeated measures ANOVA  $p < 0.05$ ), but similar or higher drug-in-nail levels at the end of the experiment (Table 3). This reflects previous reports (Kerai et al., 2016; Kerai et al., 2015) and is thought to be due to a greater affinity of terbinafine for the nail keratin (Tatsumi et al., 2002) which leads to drug accumulation in the nail plate at the expense of drug exiting the nail.

## **3.2 Influence of the chemical unguinal enhancers**

### **3.2.1 Influence of chemical enhancer inclusion on gel polymerisation and film properties**

Inclusion of water, ME, NMP and PEG 200 in the gels did not seem to adversely affect polymerisation and film formation when the gels were exposed to UVA. The extent of polymerisation, measured by the degree of alkene-to-alkane conversion, was between 58-67%, the levels of residual monomers were very low ( $\leq 1\%$  DUDMA and  $\leq 0.007\%$  HEMA) and the values were similar to those for the control formulation (Table 4). Similarly, several properties of the films were unchanged by the incorporation of water, ME, NMP or PEG 200. For example, there were no changes in film thickness or visual appearance, which remained smooth, transparent and aesthetically acceptable. FT-IR and XRD spectra and polarised light micrographs showed no obvious differences (Supplementary material 6-7) and scanning electron microscopy revealed dense film interiors (Fig. 4) similar to the control films. Presence of water, ME, NMP or PEG 200 did not influence drug loads, such that the concentrations in the films were similar to those in the uncured gels ( $p > 0.05$ , Table 4). For its part, the nature of drug did not influence the physical appearance of the film or its Tg or degree of conversion or levels of residual monomers or yield ( $p > 0.05$ ), reflecting previous reports (Kerai et al., 2015).

There were a few differences however. Films containing mercaptoethanol had significantly lower glass transition temperatures as well as increased gel-to-film mass yields (by ~16%,  $p < 0.05$ , compared to the control). Meanwhile the presence of water in the gel formulations resulted in films containing 'bubbles' (Fig. 5), which could be trapped water or air.

### **3.2.2 Influence of the penetration enhancers on drug release from the films and on unguinal drug permeation**

Inclusion of a penetration enhancer in the film did not influence the shape of the drug release profiles (burst release followed by a slower phase) or the mechanism of drug release (diffusion-controlled indicated by the high fit to the Higuchi model), or the impact of drug nature (amorolfine HCl being released to a greater extent than terbinafine HCl), but did have a significant effect on the extent of drug release (Fig. 6). Irrespective of drug nature, drug release was greatest from films containing ME, followed by PEG 200, NMP, water and the control, although statistically only the films containing ME, PEG 200 or NMP had greater drug release compared to the control (repeated measures ANOVA,  $p < 0.05$ ). At the end of the release study, all the films were intact, showed negligible change in mass and no signs of drug precipitation.

The unguinal drug permeation profiles and calculated permeation parameters are shown in Fig. 7 and Table 5 respectively. From Fig. 7, it can be seen that, for both drugs, the presence of mercaptoethanol, NMP and PEG 200 in the films increased unguinal drug permeation (repeated measures ANOVA,  $p < 0.05$  compared to the control) while the presence of water had no statistical influence (repeated measures ANOVA  $p > 0.05$  compared to the control). When all the enhancers were compared, mercaptoethanol was the most effective, increasing the flux and permeability coefficient, and reducing the lag time for amorolfine HCl, and increasing the diffusion coefficient and reducing the lag time for terbinafine HCl (Fig. 7 and Table 5). All the chemicals incorporated in the films, including water, caused a significant increase in the level of drug that was measured in the nails at the end of the 30-day permeation experiment (Table 5, also seen in inset of Fig. 7). Calculations showed mass balance to be 94-97% (shown in Supplementary material 8).

## 4. Discussion

### Influence of the nature of the lamp

We had hypothesised that the use of a UV-LED lamp emitting light at a wavelength that was suboptimal for gel curing would result in incomplete polymerisation, and a resulting film where the loaded drug would be less 'trapped', such that it would be released to a greater extent, compared to a traditional 'optimum' UV lamp. What we found was that the nature of the lamp influenced some, but not all the parameters measured. Reduced gel-to-film mass yield and thinner LED cured films resulted when a larger amount of unreacted monomer (the oxygen inhibition layer) was removed from the film's surface following gel exposure to LED-UV lamp, which indicates a larger inhibitory influence of atmospheric oxygen on polymerisation when the lamp was suboptimal. In addition to the lamp's influence at the surface of the reaction, the film's interior was also influenced, evidenced by lower T<sub>g</sub> of LED-cured films and higher levels of residual DUDMA reactants. These indicate a less complete gel curing being achieved by the UV-LED lamp, as we had hypothesised. Any difference in the amount of heat generated by the UV and UV-LED lamps was ruled out as a potential contributor to the differences in polymerisation and film properties, given that the temperatures reached within the two lamps were similar ( $p > 0.05$ , Supplementary material 9), with temperature increasing by a maximum of 3 °C by the end of the 2-minute gel curing. The differences in polymerisation and film are therefore most likely due to the fact that the light emitted by the UV-LED lamp (350-375 nm) was not optimal for the photoinitiator, whose UV absorbance peaks are at 245, 280 and 331 nm.

However, despite the UV absorbance peaks of the photoinitiator being outside the range of the LED lamp, the light emitted by the UV-LED lamp was still able to cause gel polymerisation to a sufficient extent. Consequently, the nature of the lamp did not influence the degree of alkene-to-alkane conversion, levels of residual EMA or the film's visual appearance and microstructure, uniformity of thickness, drug concentration, FT-IR

spectra and amorphous nature. The very low levels of residual EMA and DUDMA monomers in the LED-cured films indicate a low risk of allergic contact dermatitis (which can be caused by the monomers) and means that, like the traditional UV-cured films, the LED-cured films may be used in practice.

As hypothesised, greater drug release was observed from the incompletely polymerised LED-cured films, albeit this was only statistically significant for amorolfine HCl from day 15 onwards, and was modest (by 13-15% on days 15-30). Such a small effect of the lamp on drug release may be explained by the fact that, although suboptimal, the light emitted by the LED lamp was sufficient such that many of the film's properties, which can be expected to influence drug release such as the film microstructure, did not change significantly, as discussed in the preceding paragraph. The modest enhancement of drug release from LED-cured films had, in turn, a modest influence on unguinal drug permeation, with increase in some of the unguinal permeation parameters for the two drugs. This shows that modulation of gel polymerisation by the use of a suboptimal lamp is possible, but is not a very effective strategy for enhancing unguinal drug permeation, and highlights the importance of evaluating the second strategy discussed below.

### **Influence of chemical unguinal enhancers**

Water, ME, NMP and PEG 200 have boiling points of 100°C, 157°C, 202°C and >250°C respectively. As such, they are not expected to evaporate off during gel curing, and are therefore expected to remain in the film. This could explain the 'bubbles' seen in the light micrographs of the films containing water (Fig. 5), if the water was not uniformly dispersed within the film, but was concentrated into 'droplets'. Otherwise, incorporation of water, ME, NMP and PEG 200 in the gels did not adversely affect polymerisation. On the contrary, inclusion of ME seems to enhance polymerisation, resulting in an increased gel-to-film mass yield. This reflects the observation made during gel preparation (described in Section 2.2.2) that formulations containing mercaptoethanol polymerised even in the absence of UVA application. The greater gel-to-film mass yield could be due to a thinner oxygen inhibition layer formed, and subsequently removed. As mentioned above, the oxygen inhibition layer is formed due to the inhibition of polymerisation by atmospheric oxygen. The latter reacts with the initiating or propagating radicals to form peroxy radicals (Supplementary material 10) which are unreactive towards the (meth)acrylate C=C bond, and thereby terminate

polymerisation through radical-radical recombination (Odian, 1991; Rabek, 1993). Thiols are known to reduce the inhibitory effects of O<sub>2</sub> on resin formulations (Hoyle and Bowman, 2010). In the presence of initiating radicals, hydrogen transfer by the thiol provides a thiyl radical which can propagate the polymerisation reactions. Peroxyl radicals can also abstract hydrogen from thiol, and as a result reinitiation occurs by a thiyl radical and polymerisation can continue (Supplementary material 10) (Ligon et al., 2014). Participation of ME in the polymerisation reactions via thiyl radicals has a considerable influence on the polymer film formed, whose T<sub>g</sub> was significantly reduced. The thiyl radicals may be interfering with polymer cross-linking, causing greater flexibility of the polymer chains and a lower T<sub>g</sub> (Table 4).

Incorporation of the chemicals had a significant influence on drug release (Fig. 6). We speculate that the increase in drug release was caused by the unguinal enhancers' influence on the polymer network, which in this case, is indicated by their influence on the degree of alkene-to-alkane conversion (Table 4). A lower alkene-to-alkane conversion during gel polymerisation indicates lesser cross-linking in the resulting polymer, which in turn would allow greater polymer chain flexibility and greater free volume in the polymer, which would allow greater drug diffusion and drug release out of the film. Indeed a high correlation was found between degree of conversion and drug released by day 30 (Spearman's rho correlation  $r = -0.9$ ,  $p < 0.05$  for both amorolfine HCl and terbinafine HCl).

The enhanced drug release by the incorporation of chemicals was reflected in enhanced unguinal drug permeation, with similarities between the rank orders for the permeation and release profiles. This indicates that the chemicals were exerting their unguinal permeation enhancing effect, at least to some extent, via their influence on drug release. ME was the most promising enhancer, as expected from the literature. While the other chemicals, NMP, PEG 200 or water had a smaller influence on the unguinal permeation profiles, these chemicals increased drug-in-nail levels measured at the end of the permeation experiment to similar extents compared to ME ( $p > 0.05$ ). This dichotomy, i.e. similar increase in drug-in-nail levels with lower increases in drug permeation through the nail indicates that NMP, PEG 200 and water induced changes in the nailplate which caused the latter to retain the drug (rather than allowing the drug to exit out of the nail). These chemical enhancers were

therefore acting on the nailplate itself (as well as on the film). Greater drug-in-nail levels at the expense of drug flux out of the nail, shown by NMP, PEG 200 and water, may be a positive effect. High drug-in-nail levels *in vivo* could mean a drug reservoir in the nail plate, which enables a longer-term drug depot to (i) kill the fungus and any newly-germinating fungal spores residing in the nail plate, and (ii) permeate into and exert antifungal activity in the nail bed.

#### **4. Conclusions**

We set out to compare two strategies for enhancing unguinal drug permeation from UV-cured films. The first strategy – of increasing drug release from films by reducing the extent of polymerisation – had modest effects on drug release and on unguinal drug permeation. In contrast, the second strategy – of increasing unguinal drug permeability using chemicals – enhanced unguinal drug permeation considerably. Interestingly, inclusion of the chemicals also increased drug release from the films. This poses the question of whether drug permeation was enhanced via a chemical's action on the nail plate permeability or via the chemical's action on drug release from the film. Similarities in the rank orders of drug release and unguinal permeation profiles suggest that, to a certain extent, the chemical enhancers enhanced unguinal permeation via their influence on the film i.e. by enhancing drug release. However, a considerable role of the chemical enhancer's action on the nailplate itself, which led to greatly increased drug-in-nail levels, was also found. We conclude that the chemicals enhanced unguinal permeation from UV-cured films, via both their influences on the film (drug vehicle) and on the nail plate.

#### **Acknowledgements**

The authors thank UCL School of Pharmacy for funding this work and are grateful to the volunteers who donated their nail clippings used in the *in vitro* permeation studies.

## References

- Ahn, T., Lee, J.-P., Kim, J., Oh, S., Chun, M.-K., Choi, H.-K., 2013. Effect of Pressure Sensitive Adhesive and Vehicles on Permeation of Terbinafine Across Porcine Hoof Membrane. *Archives of Pharmaceutical Research* 36, 1403-1409.
- Arrese, J.E., Pierard, G.E., 2003. Treatment failures and relapses in onychomycosis: A stubborn clinical problem. *Dermatology* 207, 255-260.
- Delgado-Charro, M.B., 2015. A pharmaceuticals perspective on drug delivery to the nail: recent advances and challenges. *Therapeutic delivery* 6, 773-775.
- Draelos, Z.D., 2010. *Cosmetic Dermatology: Products and Procedures*. Wiley-Blackwell, Oxford.
- Elsayed, M.M.A., 2015. Development of topical therapeutics for management of onychomycosis and other nail disorders: A pharmaceutical perspective. *J. Controlled Release* 199, 132-144.
- Gunt, H.B., Kasting, G.B., 2007. Effect of Hydration on the Permeation of Ketoconazole Through Human Nail Plate In Vitro. *European Journal of Pharmaceutical Sciences* 32, 254-260.
- Halvorson, R.H., Erickson, R.L., Davidson, C.L., 2003. The Effect of Filler and Silane Content on Conversion of Resin-Based Composite. *Dental Materials* 19, 327-333.
- Hossin, B., 2015. *The Rational Design of an Antifungal Nail Lacquer Using the Hansen Solubility Parameter Concept*, UCL School of Pharmacy. University College London, London.
- Hossin, B., Rizi, K., Murdan, S., 2016. Application of Hansen Solubility Parameters to Predict Drug-Nail Interactions, which can Assist the Design of Nail Medicines. *European Journal of Pharmaceutics and Biopharmaceutics* 102, 32-40.
- Hoyle, C.E., Bowman, C.N., 2010. Thiol-ene Click Chemistry. *Angewandte Chemie International Edition in English* 49, 1540-1573.
- Kerai, L.V., Hilton, S., Maugueret, M., Kazi, B.B., Faull, J., Bhakta, S., Murdan, S., 2016. UV-curable gels as topical nail medicines: In vivo residence, anti-fungal efficacy and influence of gel components on their properties. *Int. J. Pharm.* 514, 244-254.
- Kerai, L.V., Hilton, S., Murdan, S., 2015. UV-curable gel formulations: Potential drug carriers for the topical treatment of nail diseases. *Int. J. Pharm.* 492, 177-190.
- Kushwaha, A., Murthy, R.N., Murthy, S.N., Elkeeb, R., Hui, X., Maibach, H.I., 2015. Emerging therapies for the treatment of unguis onychomycosis. *Drug Dev. Ind. Pharm.* 41, 1575-1581.
- Ligon, S.C., Husár, B., Wutzel, H., Holman, R., Liska, R., 2014. Strategies to Reduce Oxygen Inhibition in Photoinduced Polymerization. *Chemical Reviews* 114, 557-589.
- Milobratovic, D., Jankovic, S., Vukicevic, J., Marinkovic, J., Jankovic, J., Railic, Z., 2013. Quality of life in patients with toenail onychomycosis. *Mycoses* 56, 543-551.
- Murdan, S., 2012. The Nail: Anatomy, Physiology, Diseases, and Treatment, in: Murthy, S.N., Maibach, H. (Eds.), *Topical Nail Products and Unguis Drug Delivery*. CRC Press, Boca Raton, pp. 1-36.
- Murdan, S., 2016. Nail disorders in older people, and aspects of their pharmaceutical treatment. *Int. J. Pharm.*, in press.
- Nair, A.B., Chakraborty, B., Murthy, S.N., 2010. Effect of Polyethylene Glycols on the Trans-unguis Delivery of Terbinafine. *Current Drug Delivery* 7, 407-414.
- Odian, G., 1991. *Principles of Polymerisation*. Wiley & Sons, New York.
- Ortonne, J.P., Baran, R., Corvest, M., Schmitt, C., Voisard, J.J., Taieb, C., 2010. Development and validation of nail psoriasis quality of life scale (NPQ10). *J. Eur. Acad. Dermatol. Venereol.* 24, 22-27.
- Patel, M., Vora, Z., 2016. Formulation Development and Optimization of Transunguis Drug Delivery System of Terbinafine Hydrochloride for the Treatment of Onychomycosis. *Drug Delivery and Translational Research* 6, 263-275.
- Rabek, J.F., 1993. Experimental and Analytical Methods for the Investigation of Radiation Curing, in: Fouassier, J.P., Rabek, J.F. (Eds.), *Radiation Curing in Polymer Science and Technology*. Elsevier, London, p. 329.
- Rich, P., Scher, R.K., 2003. *An Atlas of Diseases of the Nail*. The Parthenon Publishing Group, London.

Saner, M.V., Kulkarni, A.D., Pardeshi, C.V., 2014. Insights into drug delivery across the nail plate barrier. *J. Drug Target.* 22, 769-789.

Schoon, D.D., 2005. *Nail Structure and Product Chemistry*, 2nd Edition ed. Milady, a Part of Cengage Learning, USA.

Schwalm, R., 2007. Raw Materials, in: Schwalm, R. (Ed.), *UV Coatings: Basics, Recent Developments and New Applications*, First ed. Elsevier, Oxford, pp. 95-140.

Shapiro, S.E., 2014. *Nails, The Story of the Modern Manicure*. Prestel, Munich.

Shivakumar, H.N., Juluri, A., Desai, B.G., Murthy, S.N., 2012. Ungual and Transungual drug delivery. *Drug Dev. Ind. Pharm.* 38, 901-911.

Tatsumi, Y., Yokoo, M., Senda, H., Kakehi, K., 2002. Therapeutic Efficacy of Topically Applied KP-103 against Experimental Tinea Unguium in Guinea Pigs in Comparison with Amorolfine and Terbinafine. *Antimicrobial Agents and Chemotherapy* 46, 3797-3801.

Thomas, J., Jacobson, G.A., Narkowicz, C.K., Peterson, G.M., Burnet, H., Sharpe, C., 2010. Toenail onychomycosis: an important global disease burden. *J. Clin. Pharm. Ther.* 35, 497-519.

Walters, K.A., Flynn, G.L., 1983. PERMEABILITY CHARACTERISTICS OF THE HUMAN NAIL PLATE. *International Journal of Cosmetic Science* 5, 231-246.

Williams, A.C., 2003. *Transdermal and Topical Drug Delivery*. Pharmaceutical Press, London.

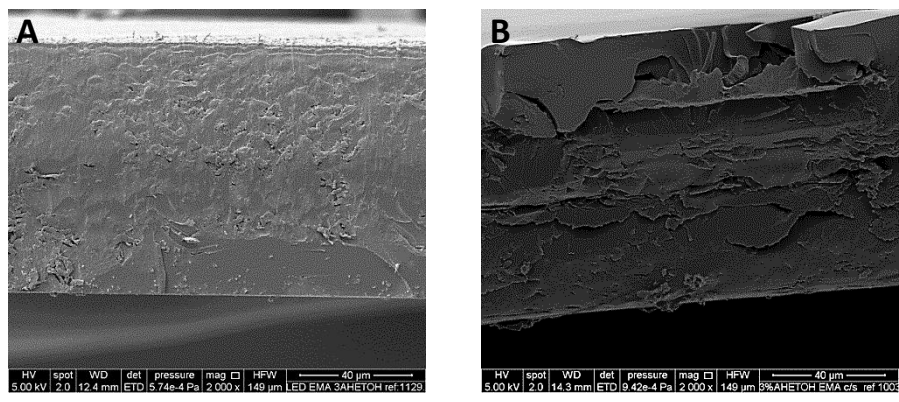


**Fig. 1** Scanning electron micrographs of the cross-sectional surfaces of amorphine HCl - loaded films produced using (A) UV-LED lamp or (B) traditional UV lamp. Terbinafine HCl - loaded films had similar scanning electron micrographs.

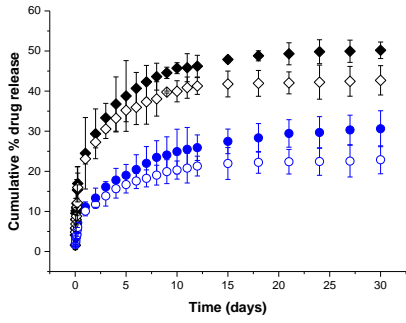


**Fig. 2** Cumulative % drug release from the films produced by the two lamps. **AH**-loaded **LED** cured film (◆); **AH**-loaded **UV** cured film (◇); **TH**-loaded **LED** cured film (●); **TH**-loaded **UV** cured film (○). Means and standard deviations are shown, n=3.

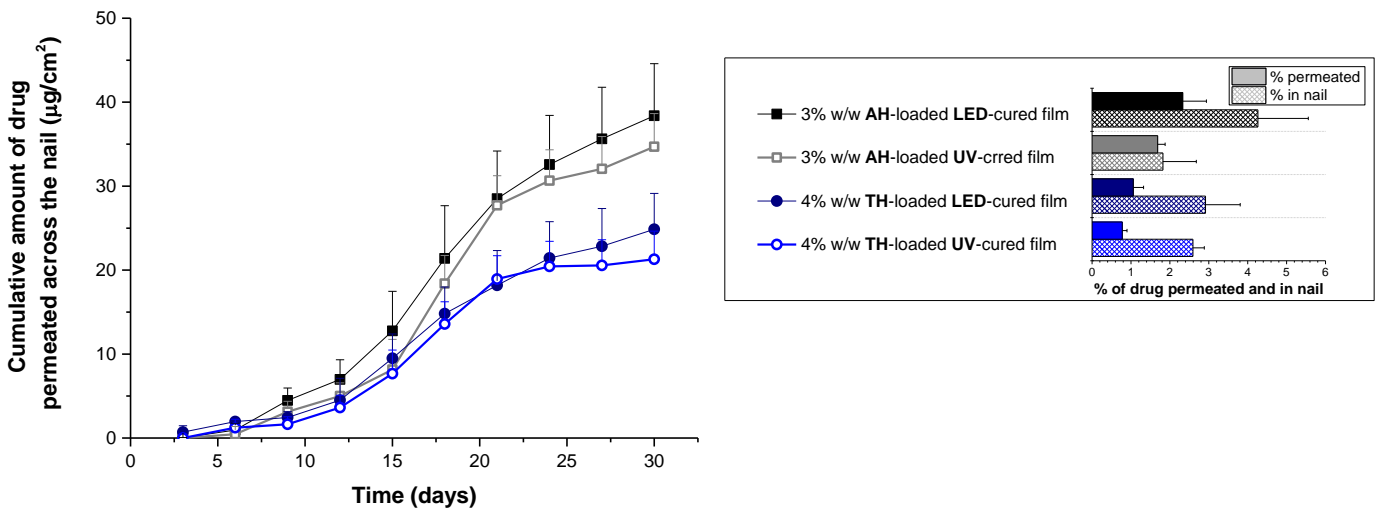


**Fig. 3** Cumulative amount of drug which permeated through the nail plate following topical application of the films produced by the two lamps. Inset shows symbols and % of the applied drug which had exited out of the nail and which remained in the nail on day 30. Means and standard deviations are shown, n=6.

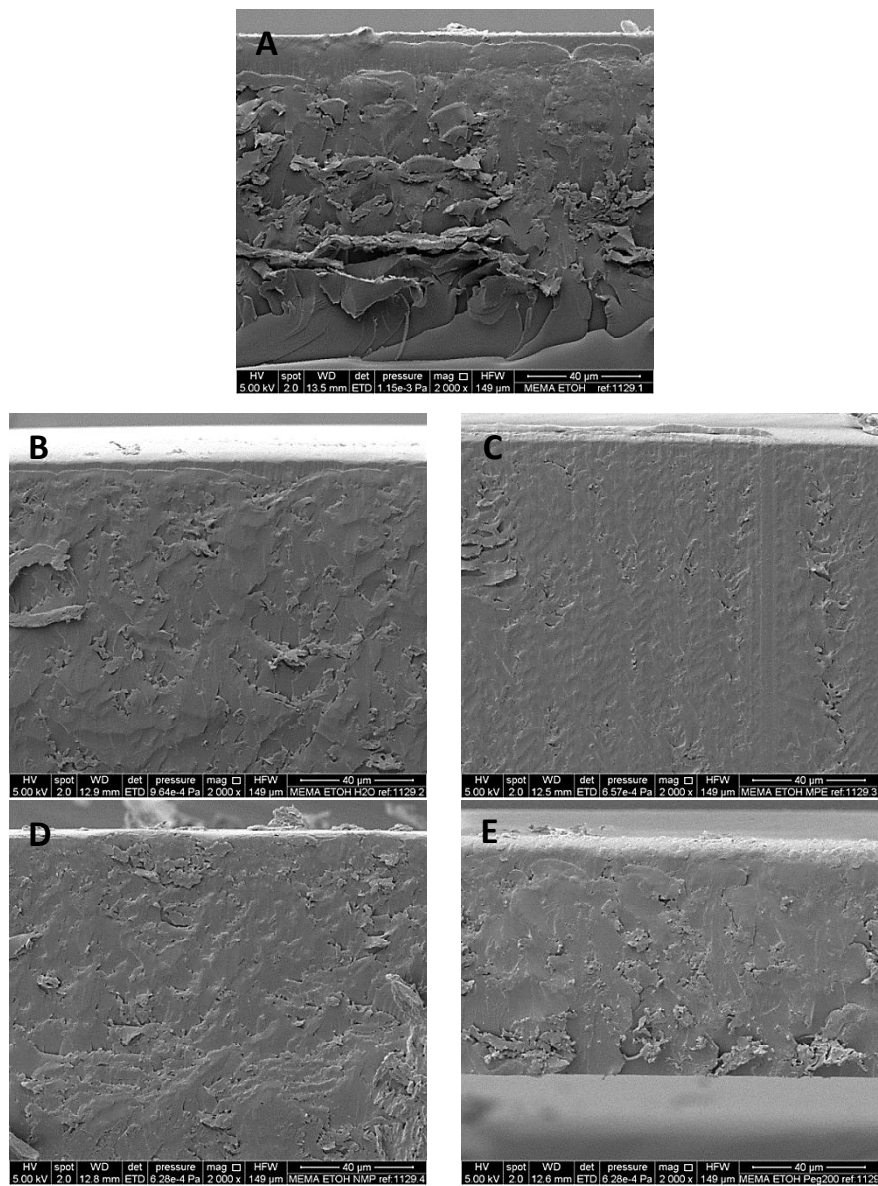


**Fig. 4** Scanning electron micrographs of the cross-sectional surfaces of UV-cured films produced from AH-loaded DUDMA & HEMA gels containing ethanol and (A) no enhancer, (B) water, (C) ME, (D) NMP and (E) PEG 200. TH-loaded gels cured produced similar scanning electron micrographs.

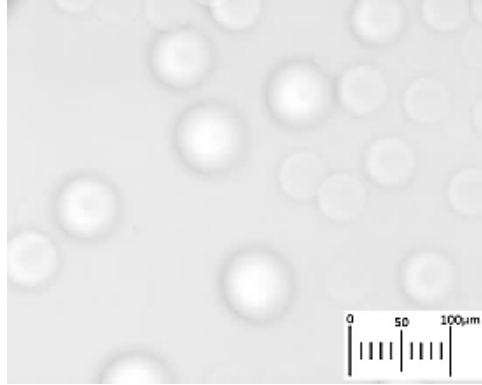


**Fig. 5** Optical micrograph of film produced from an amorphine HCl-loaded gel formulation containing water as the enhancer. The TH-loaded gels cured to produce similar films.

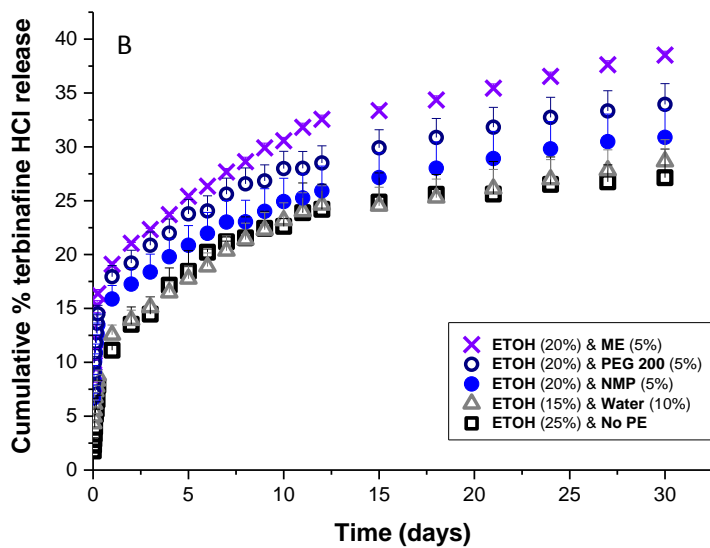
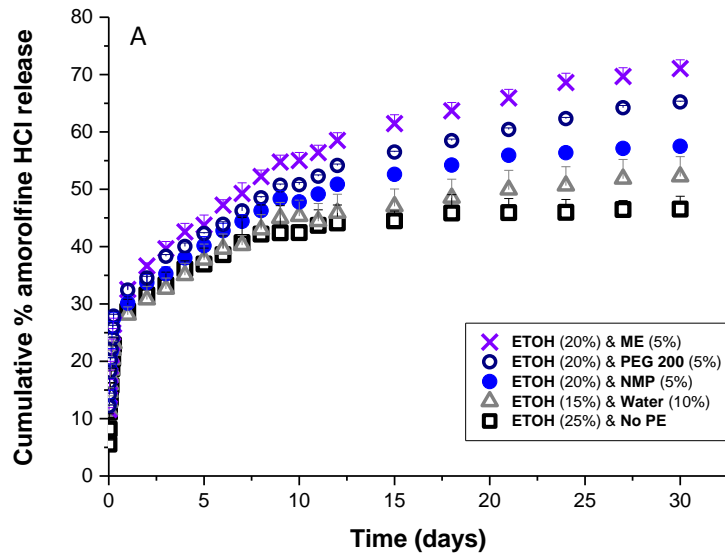


**Fig. 6** Influence of chemical enhancer inclusion on the cumulative % drug release from UV-cured films. A: amorphine HCl ; B: terbinafine HCl. Means and standard deviations are shown, n=3.

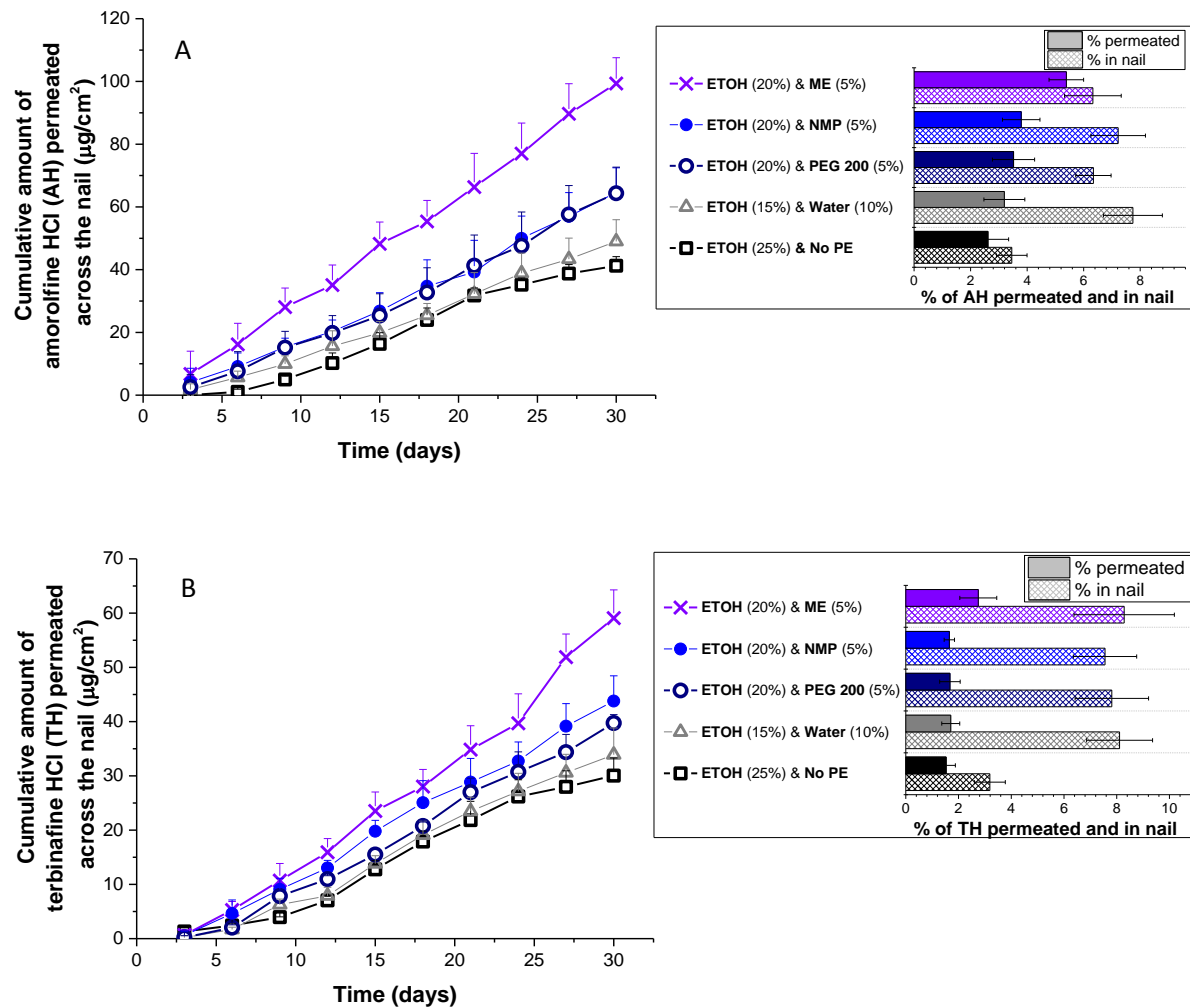


**Fig. 7** Influence of chemical enhancer inclusion on the cumulative amount of amorolfine HCl (A) or terbinafine HCl (B) that permeated through the nail from the UV-cured films. Inset shows % of the topically applied drug which permeated through the nail and which remained in the nail, i.e. drug-in-nail levels at day 30. Means and standard deviations are shown,  $n=6$ .

**Table 1. Composition of the gels incorporating unguual enhancers and drug (amorolfine HCl at 4% w/v OR terbinafine HCl at 6% w/v)**

Nature of enhancer	Amount (% v/v of the gel mixture)				
	Enhancer	Ethanol	DUDMA	HEMA	photoinitiator
None	-	25			
Water	10	15			
ME	5	20	61.2	10.8	3
NMP	5	20			
PEG 200	5	20			

**Table 2. Properties of gels and of the resulting films cured by a UV-LED or a traditional UV lamp. Means  $\pm$  sd are shown, n=3 for all, except for film thickness where n=9.**

Lamp used	Drug	Concentration of drug in gel (% w/v)	Alkene to alkane degree of conversion (%)	Concentration of residual DUDMA in film (% w/w)	Concentration of residual EMA in film (% w/w)	Gel to film mass yield (%)	Concentration of drug in film (% w/w)	Film thickness ( $\mu$ m)	Film Tg ( $^{\circ}$ C)
UV-LED	AH	3.0 $\pm$ 0.27	64.8 $\pm$ 3.9	1.0 $\pm$ 0.04*	0.004 $\pm$ 0.003	70.1 $\pm$ 2.1*	3.3 $\pm$ 0.08	133.3 $\pm$ 6.6*	100.7 $\pm$ 2.6*
Traditional UV	AH	3.0 $\pm$ 0.27	68.4 $\pm$ 0.2	0.7 $\pm$ 0.03	0.003 $\pm$ 0.00008	85.9 $\pm$ 1.9	3.3 $\pm$ 0.16	163.3 $\pm$ 8.7	109.4 $\pm$ 1.3
UV-LED	TH	4.0 $\pm$ 0.39	63.7 $\pm$ 1.5	1.0 $\pm$ 0.06*	0.006 $\pm$ 0.003	71.5 $\pm$ 3.1*	3.9 $\pm$ 0.12	135.0 $\pm$ 5.0*	98.7 $\pm$ 4.1*
Traditional UV	TH	4.0 $\pm$ 0.39	67.3 $\pm$ 2.0	0.7 $\pm$ 0.03	0.005 $\pm$ 0.002	86.5 $\pm$ 1.7	3.9 $\pm$ 0.11	164.4 $\pm$ 7.3	109.6 $\pm$ 0.8

**Table 3 Influence of the nature of the lamp on unguinal permeation parameters. Means and standard deviations are shown, n=6. \* shows statistical difference between the films produced using traditional UV or UV-LED lamp, t test, p<0.05.**

<b>Drug</b>	<b>Lamp used for polymerisation</b>	<b>Lag time (day)</b>	<b>Steady-state flux (<math>\mu\text{g}/\text{cm}^2/\text{day}</math>)</b>	<b>Permeability coefficient <math>\times 10^{-5}</math> (cm/day)</b>	<b>Diffusion coefficient <math>\times 10^{-5}</math> (<math>\text{cm}^2/\text{day}</math>)</b>	<b>Drug in nail clipping (<math>\text{mg}/\text{cm}^3</math>)</b>
<b>Amorolfine HCl</b>	<b>UV-LED</b>	8.8 $\pm$ 1.3*	2.2 $\pm$ 0.4	7.4 $\pm$ 1.4	2.7 $\pm$ 1.1	0.72 $\pm$ 0.30*
	<b>UV</b>	10.4 $\pm$ 0.9	2.4 $\pm$ 0.2	7.9 $\pm$ 0.7	2.7 $\pm$ 0.8	0.35 $\pm$ 0.18
<b>Terbinafine HCl</b>	<b>UV-LED</b>	8.2 $\pm$ 1.9	1.4 $\pm$ 0.3	3.5 $\pm$ 0.8	2.9 $\pm$ 1.0*	0.7 $\pm$ 0.2
	<b>UV</b>	9.5 $\pm$ 1.2	1.5 $\pm$ 0.1	3.7 $\pm$ 0.3	1.6 $\pm$ 0.4	0.9 $\pm$ 0.2

**Table 4. Influence of chemical enhancer incorporation on the properties of gels and of the resulting films. Means  $\pm$  sd are shown, n=3 for all, except for film thickness where n=9.**

Penetration enhancer	Drug	Concentration drug in gel (% w/v)	Mass yield (%)	Degree of conversion (%)	Film thickness ( $\mu$ m)	Concentration of drug in film (% w/w)	Film Tg ( $^{\circ}$ C)
None	AH	4.0 $\pm$ 0.49	80.8 $\pm$ 0.5	64.7 $\pm$ 1.6	163.3 $\pm$ 7.1	4.4 $\pm$ 0.04	99.2 $\pm$ 1.8
	TH	6.0 $\pm$ 0.22	80.7 $\pm$ 1.1	63.0 $\pm$ 3.2	164.4 $\pm$ 5.3	5.9 $\pm$ 0.07	94.7 $\pm$ 4.8
Water	AH	4.0 $\pm$ 0.02	85.4 $\pm$ 1.5	66.6 $\pm$ 0.8	172.2 $\pm$ 6.7	4.2 $\pm$ 0.45	103.8 $\pm$ 7.9
	TH	6.1 $\pm$ 0.08	86.6 $\pm$ 2.0	66.2 $\pm$ 4.5	174.4 $\pm$ 6.3	5.8 $\pm$ 0.23	98.2 $\pm$ 7.5
ME	AH	4.1 $\pm$ 0.28	94.0 $\pm$ 1.4	58.4 $\pm$ 1.4	181.7 $\pm$ 6.1	4.3 $\pm$ 0.31	65.8 $\pm$ 2.1
	TH	6.0 $\pm$ 0.22	93.2 $\pm$ 0.9	58.2 $\pm$ 1.2	180.6 $\pm$ 6.8	5.8 $\pm$ 0.32	64.6 $\pm$ 0.2
NMP	AH	4.0 $\pm$ 0.21	79.7 $\pm$ 1.4	63.9 $\pm$ 0.6	161.7 $\pm$ 7.1	4.4 $\pm$ 0.56	98.8 $\pm$ 0.3
	TH	6.0 $\pm$ 0.13	79.2 $\pm$ 1.5	62.8 $\pm$ 2.7	162.2 $\pm$ 7.9	5.9 $\pm$ 0.17	97.0 $\pm$ 2.3
PEG 200	AH	4.0 $\pm$ 0.36	77.5 $\pm$ 1.9	59.5 $\pm$ 2.0	158.3 $\pm$ 5.0	4.4 $\pm$ 0.34	106.1 $\pm$ 0.3
	TH	6.0 $\pm$ 0.24	77.4 $\pm$ 0.5	59.3 $\pm$ 1.3	158.9 $\pm$ 6.0	5.9 $\pm$ 0.19	103.9 $\pm$ 3.1

**Table 5. Influence of chemical enhancer inclusion on unguinal permeation parameters. Means and standard deviations are shown, n=6. \* shows statistical difference compared to the control (no enhancer) p<0.05**

Permeation enhancer	Amorolfine HCl (4%w/v in film)					Terbinafine HCl (6% w/v in film)				
	Lag time (day)	Flux ( $\mu\text{g}/\text{cm}^2/\text{day}$ )	Permeability coefficient $\times 10^{-5}$ (cm/day)	Diffusion coefficient $\times 10^{-5}$ ( $\text{cm}^2/\text{day}$ )	Drug in nail clipping ( $\text{mg}/\text{cm}^3$ )	Lag time (day)	Steady-state flux ( $\mu\text{g}/\text{cm}^2/\text{day}$ )	Permeability coefficient $\times 10^{-5}$ (cm/day)	Diffusion coefficient $\times 10^{-5}$ ( $\text{cm}^2/\text{day}$ )	Drug in nail clipping ( $\text{mg}/\text{cm}^3$ )
<b>ME</b>	1.4 $\pm$ 1.1*	3.4 $\pm$ 0.5*	8.5 $\pm$ 1.1*	24.0 $\pm$ 16.4	1.2 $\pm$ 0.3*	3.2 $\pm$ 2.3*	2.0 $\pm$ 0.4	3.3 $\pm$ 0.7	12.4 $\pm$ 8.1*	1.6 $\pm$ 0.2*
<b>NMP</b>	3.2 $\pm$ 2.8*	2.4 $\pm$ 0.6	6.0 $\pm$ 1.6	10.3 $\pm$ 8.8	1.4 $\pm$ 0.3*	3.2 $\pm$ 0.9*	1.6 $\pm$ 0.2	2.7 $\pm$ 0.3	6.6 $\pm$ 2.3	2.1 $\pm$ 0.5*
<b>PEG 200</b>	3.4 $\pm$ 3.0	2.4 $\pm$ 0.7	6.0 $\pm$ 1.8	12.8 $\pm$ 12.7	1.3 $\pm$ 0.3*	5.4 $\pm$ 1.8	1.7 $\pm$ 0.3	2.8 $\pm$ 0.5	2.8 $\pm$ 1.0	2.4 $\pm$ 0.4*
<b>Water</b>	4.4 $\pm$ 2.2	2.0 $\pm$ 0.4	4.9 $\pm$ 0.9	7.8 $\pm$ 5.2	1.1 $\pm$ 0.2*	6.6 $\pm$ 0.8	1.6 $\pm$ 0.2	2.7 $\pm$ 0.3	4.5 $\pm$ 1.3	1.5 $\pm$ 0.4*
<b>None</b>	7.1 $\pm$ 1.7	2.2 $\pm$ 0.3	5.5 $\pm$ 0.7	3.5 $\pm$ 1.4	0.6 $\pm$ 0.1	7.1 $\pm$ 1.0	1.6 $\pm$ 0.2	2.6 $\pm$ 0.4	3.0 $\pm$ 0.8	0.7 $\pm$ 0.2

**Supplementary Material**

[Click here to download Supplementary Material: Revised Murdan Supplementary material.docx](#)